Photochemical & Photobiological Sciences

PAPER

Cite this: *Photochem. Photobiol. Sci.*, 2016, **15**, 1514

Efficient organic dyes based on perpendicular 6,12-diphenyl substituted indolo[3,2-*b*]carbazole donor

Zhanhai Xiao,[a,b] Yi Di,[b] Zhifang Tan,[b] Xudong Cheng,*[a] Bing Chen*[b] and Jiwen Feng*[b]

Received 4th August 2016,
Accepted 27th October 2016

DOI: 10.1039/c6pp00286b

www.rsc.org/pps

Three novel indolo[3,2-*b*]carbazole-based dyes have been designed and synthesized using a 6,12-diphenyl substituted indolo[3,2-*b*]carbazole core as a π-conjugated donor, a thiophene cyanoacrylic acid moiety as electron acceptor and anchoring group, together with triphenylamine, 3,4,5-trimethoxybenzene and bromine as a second donor group. The photophysical and electrochemical properties of the dyes have been investigated by UV spectroscopy and cyclic voltammetry (CV). Our study indicates that the second donor plays the important role of improving dye aggregation as well as tuning the photoelectronic properties. These indolo[3,2-*b*]carbazole based dyes show good performances with high V_{oc} of 0.75 V, FF of 0.72, and a moderate PCE of 3.11% under AM 1.5 irradiation.

Introduction

Dye sensitized solar cells (DSSCs) have attracted extensive attention in recent years due to the efficient conversion of solar energy to electricity at low fabrication cost and with a relatively simple assemble technology.[1,2] In typical DSSCs, dye molecules play the key role as the light-harvesting component anchored to the surface of semiconducting TiO_2 nanocrystals. Excitation of the dye leads to the injection of electrons from the excited dye to the conduction band of the TiO_2.

To date, the most efficient class of dyes for DSSCs are ruthenium polypyridyl complexes (such as N719 and N3), which have exhibited a high energy conversion efficiency of about 11% under air mass (AM) 1.5 radiation.[3,4] However, these compounds contain expensive ruthenium metal and require careful synthesis and tricky purification steps.[5–7] Therefore, there is a strong need for substituted dyes for DSSCs containing no noble metals.

Recently, metal-free organic dyes commonly constructed with a donor–π-bridge-acceptor (D–π-A) have made great progress[8–11] due to the advantage of superior molar extinction coefficients, lower cost, and large diversity of molecular structures as well as the wide availability of their raw materials and no concern about the limited resource of noble metal ruthenium. However, the lower stability and conversion efficiency of DSSCs based on metal-free organic dyes have still to be resolved. There is an urgent need to explore new types of sensitizers with the aim of obtaining higher efficiencies of DSSCs.

In D–π-A organic dyes, intramolecular charge transfer occurs from D to A through the π-bridge unit when light is absorbed by the dyes. A crucial strategy of enhancing the efficiency of the dyes is to retain the charge separation which takes place at the interface of the dye and TiO_2. This has been demonstrated by adding hole-donating segments, such as triphenylamine and tetraphenylbenzidine, onto the ruthenium polypyridyl complexes to enhance charge separation.[12,13] To improve the absorption and charge-separation, a concept of D–D–π-A organic dyes was proposed for designing new types of sensitizers.[14–21] In these D–D–π-A structures, an additive donor unit was introduced into the dye molecule to facilitate electron transfer from the donor to the acceptor. Among various donors, triphenylamine, carbazole and their derivatives have been utilized extensively in DSSCs due to their high open-circuit photovoltage and power conversion efficiencies (PCE).[22–27]

Indolo[3,2-*b*]carbazole could be an excellent hole-donating candidate for organic dyes because of its relatively high hole mobility. In addition, compared to triphenylamine and carbazole, indolo[3,2-*b*]carbazole has a longer conjugated structure as well as higher thermal and chemical stability.[28–30] So far, few organic dyes containing an indolo[3,2-*b*]carbazole unit have been reported for DSSCs application. In this article we develop two types of organic D–D–π-A dyes bearing 6,12-diphenyl substituted indolo[3,2-*b*]carbazole, and then evaluate the potential of the indolo[3,2-*b*]carbazole core for the π-conjugated donor of metal-free organic D–D–π-A dyes. Inserting phenylene rings on the 6,12-positions of indolo[3,2-*b*]

[a]*State Key Laboratory of Advanced Technology for Materials Synthesis and Processing, Wuhan University of Technology, Wuhan 430070, People's Republic of China*

[b]*State key Laboratory of Magnetic Resonance and Atomic and Molecular Physics, Wuhan Institute of Physics and Mathematics, Chinese Academy of Science, Wuhan 430071, People's Republic of China. E-mail: chenbing@wipm.ac.cn*

carbazole has the advantage of suppressing the dye's aggregation. Finally, these novel dyes have been successfully used as sensitizers to the nanocrystalline TiO_2 based DSSCs and their corresponding photovoltaic characteristics are also presented.

Experimental

Materials

Indole and 4-bromobenzaldehyde were purchased from J&K Chemical, Ltd and used as received. Other commercially available chemical reagents were used as received without further purification. Organic solvents were purified using standard processes. All reactions were carried out under the protection of inert atmosphere.

Characterization and device fabrication

^{1}H NMR spectra and ^{13}C NMR spectra were recorded on a Bruker 500 MHz spectrometer in deuterated chloroform and DMSO solution, with tetramethylsilane as the internal reference. High-resolution mass spectrometry spectra were obtained on a Bruker microTOF-Q instrument. UV-visible absorption spectra were recorded on an HP 8453 spectrophotometer. Fluorescence spectra were measured by using a Hitachi F-4500 fluorescence spectrophotometer with the excitation at 380 nm. Cyclic voltammetry (CV) data were measured on a CHI604D electrochemical workstation, using tetrabutylammonium hexafluorophosphate (Bu_4NPF_6, 0.1 M in tetrahydrofuran) as electrolyte with scan rate of 50 mV s^{-1} at room temperature under the protection of argon. A platinum electrode was used as the working electrode, Pt wire as the counter electrode, and Ag wire as the reference electrode. At the end of the measurement, the ferrocene/ferrocium potential was measured and used as the reference.

Device fabrication followed the process employed in the literature. A transparent conductive glass, fluorine-doped SnO_2 (FTO, 2.2 mm thick, transmission >90% in the visible, sheet resistance 15 Ω per square) was used as the substrate for the fabrication of DSSCs. Mesoporous TiO_2 films were deposited by screen printing the TiO_2 nanoparticles (20 nm) over the conductive side of the FTO. The film was sintered at 500 °C for 30 min, followed by cooling to 80 °C and immersing into a dye solution of 0.3 mM in THF for 12 h at room temperature. The dye-coated TiO_2 films were used as electrodes and placed on the top of Pt-sputtered FTO glass counter electrodes. The redox electrolyte composed of 0.6 M BMII (1-butyl-3-methylimidazolium iodide), 0.05 M LiI, 0.03 M I_2, 0.5 M 4-*tert*-butylpyridine, and 0.1 M guanidinium thiocyanate in a mixture of acetonitrile–valeronitrile (85 : 15, v/v) was introduced into the interelectrode space by capillary force.

Current–voltage (*J*–*V*) characteristics of DSSCs under illumination were measured by a Keithley source meter and solar simulator coupled with a 150 W xenon lamp and an AM optical filter to give 100 mW cm^{-2} illumination at the DSSCs surface. Electrochemical Impedance spectra (EIS) in the dark were recorded using an electrochemical workstation (CHI660C) with a frequency response analyzer. Electrochemical impedance spectroscopy data were analyzed using Z-View software with an appropriate equivalent circuit. Incident photon to current conversion efficiency (IPCE) data were obtained as a function of different wavelengths by using a xenon lamp, a monochromator, and a Keithley source meter under constant illumination intensity at each wavelength. Intensity calibration for IPCE data was performed using a standard silicon photodiode.

Synthesis

6,12-Bis(4-bromophenyl)-5,11-dihydroindolo[3,2-*b*]carbazole (1). To a solution of indole (0.35 g, 3 mmol) and 4-bromobenzaldehyde (0.56 g, 3 mmol) in acetonitrile (15 mL), HI (57%) (0.26 mL, 2.0 mmol) was added at room temperature. The reaction mixture was heated at 80 °C for 14 hours and the formed precipitated was filtered off and washed with cold acetonitrile (10 mL) and carefully dried *in vacuo*. To the suspension of the mixture in acetonitrile (10 mL), iodine (0.09 g, 0.36 mmol) was added. The reaction mixture was heated at 80 °C for 14 hours. After the organic solvent was concentrated to 15 mL, the precipitate was filtered off, washed with cold acetonitrile (10 mL) and carefully dried *in vacuo*. Compound **1** was isolated by silica gel column chromatography with petroleum ether and dichloromethane (1/1, v/v) as the eluent (yield 80%). ^{1}H NMR (500 MHz, DMSO, δ, ppm): 10.63(s, 2H), 7.89(d, 4H, J = 8.34 Hz), 7.63(d, 4H, J = 8.30 Hz), 7.40(d, 2H, J = 8.07 Hz), 7.24–7.27(t, 2H, J = 7.62 Hz), 7.10(d, 2H, J = 7.90 Hz), 6.85–6.88(t, 2H, J = 7.60 Hz). ^{13}C NMR (125 MHz, $CDCl_3$, δ ppm): 141.6, 136.4, 133.9, 132.1, 125.3, 122.4, 121.5, 120.0, 117.7, 115.7, 110.7. HRMS: m/z calculated for $C_{30}H_{18}Br_2N_2$, 563.9837; found 563.9841. Elemental analysis calculated for $C_{30}H_{18}Br_2N_2$: C 63.63; H 3.20; N 4.95; found: C 63.42; H 3.37; N 4.73.

6,12-Bis(4-bromophenyl)-5,11-bis(2-ethylhexyl)-5,11-dihydroindolo[3,2-*b*]carbazole (2). To a solution of compound **1** (0.5 g, 0.91 mmol) in DMSO (20 mL), benzyltriethylammonium chloride (63 mg, 0.28 mmol) and 2-ethylhexyl bromide (0.20 g, 1.09 mmol) were added. Then the NaOH aqueous solution (50%) (1.5 mL) was dropped into the reaction mixture at room temperature. The reaction mixture was heated at 50 °C overnight under argon. Water was added to the reaction and the product isolated by filtration. The product was then washed with 50 mL water and carefully dried *in vacuo*. Compound **2** was isolated by silica gel column chromatography with petroleum ether and dichloromethane (10/1, v/v) as the eluent, yield 80%. ^{1}H NMR (500 MHz, DMSO, δ, ppm): 7.91(t, 4H, J = 7.22 Hz), 7.62–7.67(m, 4H), 7.49(d, 2H, J = 8.22 Hz), 7.32(t, 2H, J = 7.67 Hz), 6.83(t, 2H, J = 7.59 Hz), 6.40(d, 2H, J = 8.03 Hz), 3.86(dd, 4H, J = 5.6 Hz), 1.57–1.63(m, 2H), 0.80–1.09(m, 16H), 0.72–0.75(m, 6H), 0.59(t, 6H, J = 7.54 Hz). ^{13}C NMR (125 MHz, $CDCl_3$, δ ppm): 143.3, 137.8, 133.2, 133.0, 132.2, 132.1, 125.3, 122.4, 118.1, 116.9, 109.4, 48.4, 39.3, 30.1, 28.2, 23.1, 14.0, 10.5. HRMS: m/z calculated for $C_{46}H_{50}Br_2N_2$, 788.2341; found 788.2325. Elemental analysis calculated for $C_{46}H_{50}Br_2N_2$: C 69.87; H 6.37; N 3.54; found: C 69.51; H 6.48; N 3.49.

5-(4-(12-(4-Bromophenyl)-5,11-bis(2-ethylhexyl)-5,11-dihydroindolo[3,2-*b*]carba-zol-6-yl)phenyl)thiophene-2-carbaldehyde (3). Under an argon atmosphere, a mixture of compound **2** (0.53 g, 0.73 mmol), 5-bromothiophene-2-carbaldehyde (0.14 g, 0.88 mmol), $Pd(PPh_3)_4$ (0.08 g, 0.073 mmol), Na_2CO_3 (0.35 g, 3.29 mmol), THF (20 mL), and water (2 mL) was stirred and heated at 70 °C for 15 h. When the reaction was complete, the mixture was extracted with CH_2Cl_2 three times. The combined organic solution was dried with anhydrous sodium sulfate. The solvent was removed with a rotary evaporator, and the residue was isolated by silica gel column chromatography with petroleum ether and ethyl acetate (10/1, v/v) as the eluent to give compound **3**, yield 50%. ^{1}H NMR (500 MHz, DMSO, δ, ppm): 9.99(s, 1H), 8.16(d, 3H, J = 4.25 Hz), 8.00(d, 1H, J = 4.15 Hz), 7.89–7.91(m, 2H), 7.76–7.8(m, 2H), 7.62–7.67(m, 2H), 7.48(d, 2H, J = 8.38 Hz), 7.28–7.33(m, 2H), 6.77–6.84(m, 2H), 6.50(d, 1H, J = 8.21 Hz), 6.40(d, 1H, J = 8.02 Hz), 3.88(dd, J = 7.69 Hz, 4H), 1.60–1.65(m, 2H), 0.82–1.11(m, 16H), 0.74–0.79 (m, 6H), 0.60(t, 6H, J = 7.54 Hz). ^{13}C NMR (125 MHz, $CDCl_3$, δ ppm): 182.7, 153.9, 143.4, 142.7, 140.8, 138.8, 137.5, 133.1, 132.8, 132.6, 131.4, 129.0, 128.3, 126.6, 125.1, 124.4, 122.8, 122.1, 118.6, 117.8, 116.8, 109.4, 109.2, 48.4, 39.1, 30.0, 28.1, 23.0, 14.0, 10.5. HRMS: m/z calculated for $C_{51}H_{53}BrN_2OS$, 820.3062; found 820.3048. Elemental analysis calculated for $C_{51}H_{53}BrN_2OS$: C 74.52; H 6.50; N 3.41; S 3.90; found: C 74.18; H 6.59; N 3.37; S 3.82.

5-(4-(5,11-Bis(2-ethylhexyl)-12-(3′,4′,5′-trimethoxy-[1,1′-biphenyl]-4-yl)-5,11-dihydroindolo[3,2-*b*]carbazol-6-yl)phenyl)thiophene-2-carbaldehyde (4). Under argon atmosphere, to a mixture of compound **3** (0.15 g, 0.18 mmol), (3,4,5-trimethoxyphenyl) boronic acid (0.05 g, 0.22 mmol), $Pd(PPh_3)_4$ (0.02 g, 0.018 mmol) and Na_2CO_3 (0.09 g, 0.81 mmol), a mixed solution of toluene (5 mL), ethanol (2 mL) and water (0.4 mL) was added. The mixture was then stirred and heated at 70 °C for 15 h. When the reaction was complete, the mixture was extracted with CH_2Cl_2 three times. The combined organic solution was dried with anhydrous sodium sulfate. The solvent was removed with a rotary evaporator, and the residue was isolated by silica gel column chromatography with petroleum ether and ethyl acetate (5/1, v/v) as the eluent to give compound **4**, yield 65%. ^{1}H NMR (500 MHz, DMSO, δ, ppm): 10.00(s, 1H), 8.16–8.18(m, 3H), 8.08–8.09(d, 2H, J = 7.91 Hz), 8.00–8.01 (d, 1H, J = 3.86 Hz), 7.78–7.82(m, 2H), 7.71–7.76(m, 2H), 7.46–7.49(m, 2H), 7.31(t, 2H, J = 7.33 Hz), 7.17(s, 2H), 6.76–6.80(m, 2H), 6.52–6.56(m, 2H), 3.95(s, 6H), 3.91(t, 4H, J = 6.41 Hz), 3.76(s, 3H), 1.65–1.71(m, 2H), 0.79–0.96 (m, 16H), 0.55–0.63(m, 12H). ^{13}C NMR (125 MHz, $CDCl_3$, δ ppm): 182.5, 156.4, 155.2, 153.3, 147.7, 143.3, 141.0, 139.3, 137.5, 136.8, 135.3, 132.2, 131.8, 129.7, 127.4, 126.3, 125.5, 109.4, 104.4, 61.3, 56.5, 48.4, 39.2, 30.4, 28.4, 23.2, 14.8, 10.5. HRMS: m/z calculated for $C_{60}H_{64}N_2O_4S$, 908.4587; found 908.4593. Elemental analysis calculated for $C_{60}H_{64}N_2O_4S$: C 79.26; H 7.09; N 3.08; S 3.53; found: C 78.95; H 7.15; N 3.01; S 3.44.

5-(4-(12-(4′-(Diphenylamino)-[1,1′-biphenyl]-4-yl)-5,11-bis(2-ethylhexyl)-5,11-dihydroindolo[3,2-*b*]carbazol-6-yl)phenyl) thiophene-2-carbaldehyde (5). Under an argon atmosphere, a mixture of compound **3** (0.14 g, 0.17 mmol), (4-(diphenylamino) phenyl)boronic acid (0.06 g, 0.2 mmol), $Pd(PPh_3)_4$ (0.02 g, 0.017 mmol) and Na_2CO_3 (0.08 g, 0.77 mmol) in a mixed solution of toluene (5 mL), ethanol (2 mL) and water (0.4 mL) was stirred and heated at 70 °C for 15 h. When the reaction was complete, the mixture was extracted with CH_2Cl_2 three times. The combined organic solution was dried with anhydrous sodium sulfate. The solvent was removed with a rotary evaporator, and the residue was isolated by silica gel column chromatography with petroleum ether and ethyl acetate (5/1, v/v) as the eluent to give compound **5**, yield 63%. ^{1}H NMR (500 MHz, DMSO, δ, ppm): 10.00(s, 1H), 8.16–8.18 (m, 2H), 8.00–8.01(m, 3H), 7.85(d, 2H, J = 8.68 Hz),7.79–7.82 (m, 2H), 7.71(t, 2H, J = 8.20 Hz), 7.48(d, 2H, J = 8.44 Hz), 7.36–7.39(m, 4H), 7.30(m, 2H, J = 7.24 Hz), 7.10–7.17(m, 8H), 6.76–6.81(m, 2H), 6.53(t, 2H, J = 7.24 Hz), 3.91(t, 4H, J = 8.40 Hz), 1.64–1.71(m, 2H), 0.76–0.95(m, 16H), 0.55–0.62(m, 12H). ^{13}C NMR (125 MHz, $CDCl_3$, δ ppm): 182.8, 156.2, 154.7, 147.8, 147.5, 143.4, 140.8, 140.5, 139.2, 138.6, 137.1, 135.6, 134.1, 133.5, 133.0, 132.3, 132.1, 131.3, 129.3, 127.4, 126.8, 125.6, 124.5, 124.8, 123.1, 122.8, 122.3, 122.1, 48.4, 39.2, 30.1, 28.6, 23.4, 14.0, 10.5.HRMS: m/z calculated for $C_{69}H_{67}N_3OS$, 985.5005; found 985.4992. Elemental analysis calculated for $C_{69}H_{67}N_3OS$: C 84.02; H 6.85; N 4.26; S 3.25; found: C 83.77; H 6.96; N 4.22; S 3.17.

Compound ICZ-TMOP. To a stirred solution of compound **4** (0.11 g, 0.12 mmol), cyanoacetic acid (0.33 g, 0.36 mmol) and chloroform (5 mL), piperidine (0.77 g, 0.84 mmol) were added. The reaction mixture was refluxed under argon for 12 h and then acidified with 2 M hydrochloric acid aqueous solution (10 mL). The crude product was extracted into chloroform, washed with water, and dried over anhydrous sodium sulfate. After removal of the solvent under reduced pressure, the residue was purified by flash chromatography with chloroform and methanol/chloroform (1/10, v/v) in turn as eluent to yield a purple powder, yield 85% (103 mg). ^{1}H NMR (500 MHz, DMSO, δ, ppm): 10.01(s, 1H), 8.27(s, 1H), 8.10(d, 4H, J = 7.93 Hz), 7.91(t, 2H, J = 3.78 Hz), 7.71–7.80(m, 4H), 7.48(d, 2H, J = 7.12 Hz), 7.31(t, 2H, J = 7.59 Hz), 7.17(s, 2H), 6.77–6.82(m, 2H), 6.56(s, 2H), 3.96(s, 6H), 3.91–3.93(m, 4H), 3.76(s, 3H), 1.66–1.72(m, 2H), 0.56–0.64(m, 12H). ^{13}C NMR (125 MHz, $CDCl_3$, δ ppm): 167.1, 155.1, 153.7, 147.7, 143.3, 141.0, 139.9, 137.8, 136.8, 135.1, 133.1, 132.5, 131.8, 129.9, 127.4, 126.8, 125.1, 109.4, 104.4, 61.1, 56.3, 48.4, 39.3, 30.2, 28.2, 23.4, 14.0, 10.5. HRMS: m/z calculated for $C_{63}H_{65}N_3O_5S$, 975.4645; found 975.4657. Elemental analysis calculated for $C_{63}H_{65}N_3O_5S$: C 77.51; H 6.71; N 4.30; S 3.28; found: C 77.18; H 6.93; N 4.33; S 3.20.

Compound ICZ-TPA. Compound **ICZ-TPA** was synthesized from compound **5** similarly to that described for compound **ICZ-TMOP**, yield 88% (100 mg). ^{1}H NMR (500 MHz, DMSO, δ, ppm): 10.01(s, 1H), 8.30(s, 1H), 8.08(d, 2H, J = 7.51 Hz), 7.99 (d, 2H, J = 8.41 Hz), 7.92(s, 1H), 7.84(d, 2H, J = 8.65 Hz), 7.75–7.78(m, 2H), 7.70(t, 2H, J = 8.35 Hz), 7.46–7.48(m, 2H), 7.36–7.39(m, 4H), 7.30(t, 2H, J = 7.31 Hz), 7.10–7.16(m, 8H), 6.75–6.81(m, 2H), 6.51–6.56(m, 2H), 3.90(t, 4H, J = 7.95 Hz),

1.60–1.65(m, 2H), 0.76–0.96(m, 16H), 0.55–0.62(m, 12H). ^{13}C NMR (125 MHz, $CDCl_3$, δ ppm): 167.6, 154.7, 147.6, 147.5, 143.3, 140.8, 140.2, 139.8, 137.1, 135.2, 134.5, 133.2, 133.0, 132.6, 132.4, 131.8, 129.3, 127.8, 126.8, 125.2, 124.5, 124.7, 123.1, 122.8, 122.5, 122.1, 48.4, 39.3, 30.1, 28.2, 23.1, 14.0, 10.5. HRMS: *m/z* calculated for $C_{72}H_{68}N_4O_2S$, 1052.5063; found 1052.5087. Elemental analysis calculated for $C_{72}H_{68}N_4O_2S$: C 82.09; H 6.51; N 5.32; S 3.04; found: C 81.68; H 6.73; N 5.22; S 3.11.

Compound ICZ-Br. Compound **ICZ-Br** was synthesized from compound **3** similarly to that described for compound **ICZ-TMOP**, yield 83% (107 mg). ^{1}H NMR (500 MHz, DMSO, δ, ppm): 10.01(s, 1H), 8.47(s, 1H), 8.05(d, 2H, J = 7.51 Hz), 7.95 (d, 1H, J = 8.41 Hz), 7.92–7.84(m, 2H), 7.67–7.70(m, 7H), 7.75–7.78(m, 2H), 7.35(t, 4H, J = 8.35 Hz), 6.68(d, 1H, J = 7.83), 6.48(d, 1H, J = 7.75), 3.91(t, 4H, J = 7.97 Hz), 1.61–1.67(m, 2H), 0.73–0.98(m, 16H), 0.56–0.65(m, 12H). ^{13}C NMR (125 MHz, $CDCl_3$, δ ppm): 166.4, 154.9, 147.6, 143.3, 140.9, 139.8, 138.7, 135.1, 133.1, 132.6, 132.4, 131.4, 129.4, 128.9, 128.2, 126.8, 125.1, 124.8, 122.8, 122.0, 117.8, 116.7, 115.8, 48.4, 39.1, 29.3, 28.1, 23.0, 14.0, 10.5. HRMS: *m/z* calculated for $C_{54}H_{54}BrN_3O_2S$, 887.3120; found 887.3147. Elemental analysis calculated for $C_{54}H_{54}BrN_3O_2S$: C 72.96; H 6.12; N 4.73; S 3.61; found: C 72.58; H 6.34; N 4.66; S 3.51.

Results and discussion

Design and synthesis of dyes

The synthetic routes of dyes are shown in Scheme 1. Compound **1** was synthesized according to the literature. Compounds **3**, **4** and **5** were synthesized by the Suzuki-type aryl–aryl coupling reaction between the aryl boronic acid and the aryl halides.

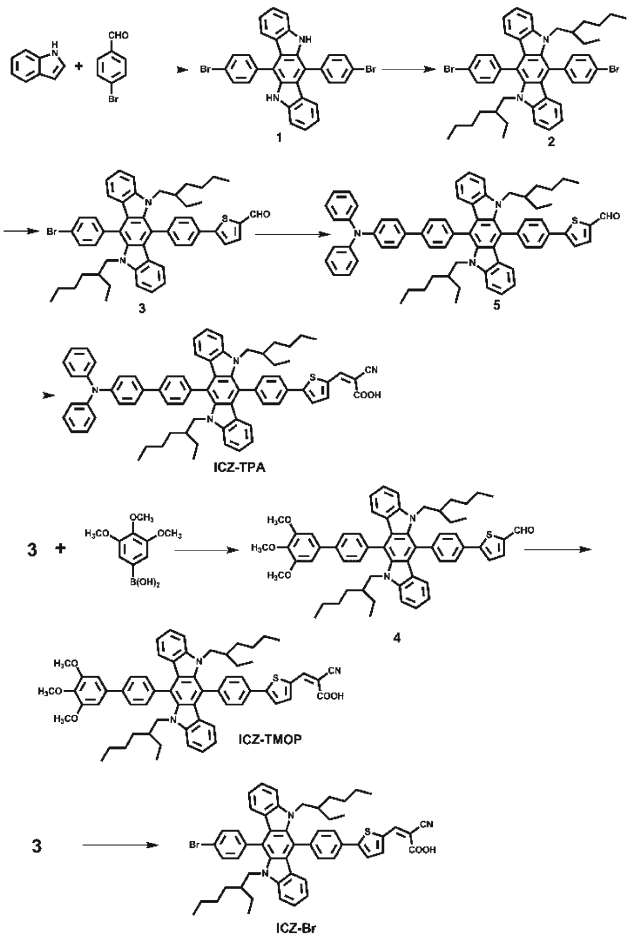

Scheme 1 Synthetic routes for the dyes.

UV-vis absorption spectra

The UV-vis absorption and fluorescence emission spectra for the dyes and the reference compound **2** were measured in DCM solutions at a concentration of 1×10^{-5} M, as presented in Fig. 1. The corresponding data were presented in Table 1. The reference compound **2** shows two major absorption bands at about 338 nm and 420 nm, which can be attributed to the localized π–π* transition of the conjugated aromatic rings. The chance of formation of intramolecular charge transfer (ICT) in compound **2** is nearly zero because of its symmetrical structure, without an obvious electron-withdrawing group. As shown in Fig. 1, the introduction of electron-withdrawing and electron-rich groups in the dyes obviously enhances the absorption of the π–π* transition bands, and produces a red-shift transition around 450 nm with a molar extinction coefficient of about 10^3 M^{-1} cm^{-1}, which may be attributed to the ICT transition. The band gaps of the dyes for **ICZ-Br**, **ICZ-TPA** and **ICZ-TMOP** estimated from the onset of the absorption spectra are 2.78, 2.66 and 2.74 eV, respectively.

In a comparison of the spectra of the dyes, **ICZ-TPA** shows the strongest absorption that can be attributed to the increase

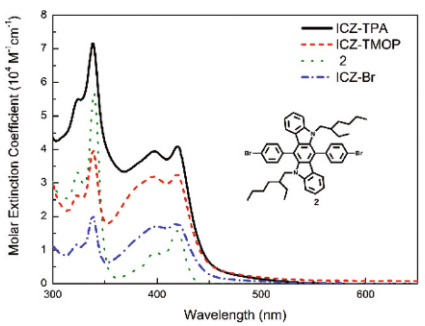

Fig. 1 UV-vis absorption and of dyes **ICZ-Br**, **ICZ-TPA** and **ICZ-TMOP** in DCM.

in the number of phenylene rings in the triphenylamine unit. This is also consistent with the result of the stronger electron-donating ability of triphenylamine than trimethoxyphenyl and bromine, which increases the light absorption intensity. Although the structure of the second donor group changed, these dyes show a little difference for the ICT absorption band. This suggests that the enhanced light absorption stems mainly from the π–π* transition absorption, not from the ICT effect.

Table 1 UV-vis absorption and electrochemical properties of the dyes

Dye	Absorption λ_{max} [a] nm/ε[a] M^{-1} cm^{-1}	E_{0-0} [b] eV	E_{ox} [c] V	E_{red} [d] V	G_{inj} [e] eV	G_{reg} [f] eV
ICZ-Br	339(2.02×10^4), 399(1.71×10^4), 420(1.8×10^4)	2.78	1.09	−1.69	−1.19	−0.69
ICZ-TPA	339(7.15×10^4), 397(3.94×10^4), 419(4.1×10^4)	2.66	1.07	−1.59	−1.09	−0.67
ICZ-TMOP	339(3.96×10^4), 397(3.19×10^4), 419(3.3×10^4)	2.74	1.12	−1.62	−1.12	−0.72

[a] Absorption peaks (λ_{max}) and molar extinction coefficients (ε) were measured in DCM solutions (1×10^{-5} M). [b] E_{0-0} was estimated from the onset of the absorption spectra in DCM solution. [c] The onset oxidative potential *versus* the normal hydrogen electrode E_{ox} [V] = E_{ox} (*vs.* Fc/Fc^+) + 0.63. [d] E_{red} [V] = $E_{ox} - E_{0-0}$. [e] Driving force for electron injection from the dye excited singlet state into the CB of TiO_2 (−0.5 V *vs.* NHE). [f] Driving force for dye regeneration by the I^-/I_3^- redox shuttle (+0.4 V *vs.* NHE).

That may be due to the large steric hindrance between the indolo[3,2-*b*]carbazole group and the adjacent phenylene rings, which largely destroys the molecular conjugation, thus deceasing the efficiency of the ICT process.

The maximal molar extinction coefficients of **ICZ-Br**, **ICZ-TPA** and **ICZ-TMOP** are about 1.8×10^4 M^{-1} cm^{-1}, 4.1×10^4 M^{-1} cm^{-1} and 3.3×10^4 M^{-1} cm^{-1}, respectively, which are higher than that of the standard N719 dye 1.4×10^4 M^{-1} cm^{-1}.[31,32] The greater molar extinction coefficients of the organic dyes allow a thinner TiO_2 film, which benefits the electrolyte diffusion in the film and reduces the recombination of the light-induced charges during transportation. The high molar extinction coefficient of our dyes suggests that the incorporation of indolo[3,2-*b*]carbazole as a π-conjugated donor in D–D–π-A organic dyes could be a good approach to improve the light absorption ability.

The fluorescence spectra of the dyes show similar behaviour (Fig. 2). Compared with **ICZ-TMOP**, **ICZ-TPA** displays a broader and red-shift emission in DMF, suggesting that the stronger electron-donating ability of triphenylamine reflects the dye conjugation. In addition, the fluorescence spectra of **ICZ-TPA** and **ICZ-TMOP** significantly red-shift with increasing solvent polarity, indicative of the CT character of the fluorescent state.

The absorption spectra of the dyes on TiO_2 films were also measured (Fig. 3). The dyes show transition absorption peaks at 416 nm, a slight blue-shift with respect to the solution, which is indicative of partial deprotonation of the carboxylic acid acceptor because of the interaction between the dye molecules and the TiO_2 film.[33] In comparison with **ICZ-TMOP** and **ICZ-TPA**, the absorption spectra of **ICZ-Br** are broader, suggesting severe dye aggregation on the TiO_2 film, which might be caused by the smaller steric hindrance of the bromine substituent in **ICZ-Br**.

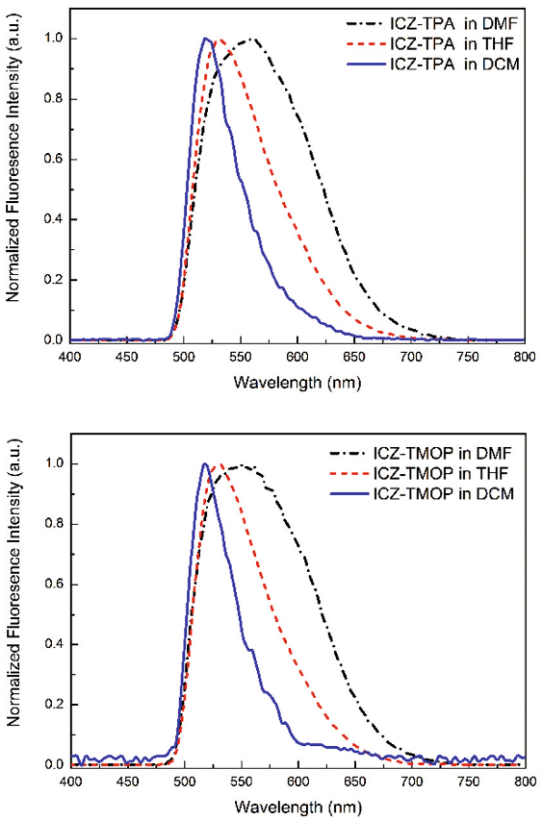

Fig. 2 Fluorescence spectra of **ICZ-TPA** and **ICZ-TMOP** in different solutions.

Electrochemical properties

Cyclic voltammetry (CV) was performed to measure the ground state oxidation potential (E_{ox}) of the dyes in THF solution with 0.1 M Bu_4NPF_6 as the electrolyte (Fig. 4). As can be seen, the voltammograms of all dyes show reversible oxidation waves, indicating stable electrochemical properties. The onset oxidative potential of ground state **ICZ-TPA** (1.07 V *versus* the normal hydrogen electrode (NHE)) is shifted in the negative direction by 0.05 V with respect to that of **ICZ-TMOP** (1.12 V), suggesting the higher electron-donating ability of triphenylamine as compared to that of trimethoxyphenylene. The oxidative potentials of the dyes in the ground states are higher than the iodine redox potential (+0.4 V),[34] which ensures fast dye regeneration and avoids the charge recombination between the oxidized dye molecules and photoinjected electrons in the TiO_2 film.

The oxidation potential levels of the excited state dyes **ICZ-Br**, **ICZ-TPA** and **ICZ-TMOP** are about 1.09, 1.07 and 1.12 V (*vs.* NHE), respectively, which are more positive than the iodine/iodide redox potential value (+0.4 V *vs.* NHE). This

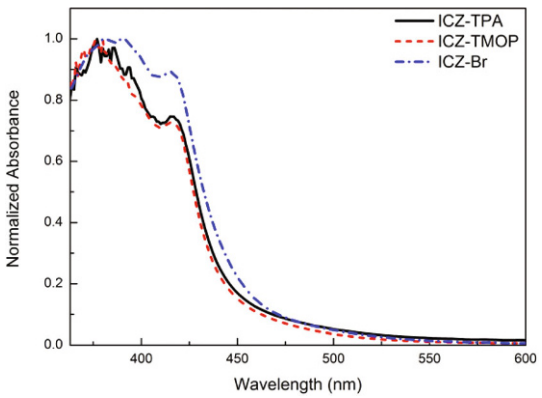

Fig. 3 UV-vis absorption spectra of **ICZ-Br**, **ICZ-TPA** and **ICZ-TMOP** adsorbed on TiO_2 films.

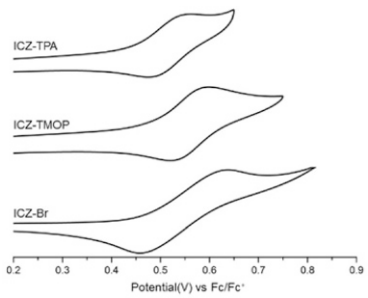

Fig. 4 Cyclic voltammograms of **ICZ-Br**, **ICZ-TPA** and **ICZ-TMOP** in THF solutions.

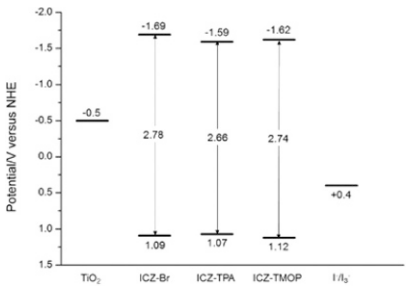

Fig. 5 Schematic energy levels of **ICZ-Br**, **ICZ-TPA** and **ICZ-TMOP** based on absorption and electrochemical data.

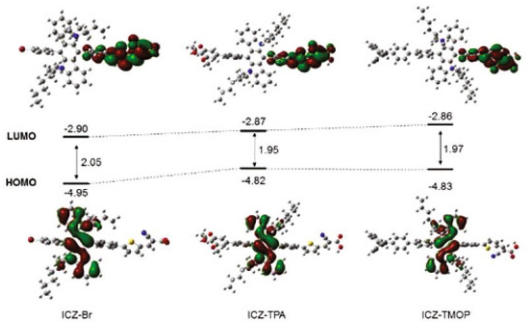

Fig. 6 Electron density distribution in the molecular orbitals of **ICZ-Br**, **ICZ-TPA** and **ICZ-TMOP**.

proves that the oxidized dyes are produced upon electron injection to TiO_2 and could therefore accept electrons from the iodide ions thermodynamically. The reductive potentials of **ICZ-Br**, **ICZ-TPA** and **ICZ-TMOP** are −1.69, −1.59 and −1.62 V (*vs.* NHE), respectively, and are more negative than the conduction-band edge of TiO_2. The driving forces for electron injection (G_{inj}) from the dye's excited singlet state into the conduction band (CB) of TiO_2 (−0.5 V *vs.* NHE) and for reduction of the dye's radical cation (G_{reg}) by the I^-/I_3^- redox couple (+0.4 V *vs.* NHE) were also calculated according to the literature.[35,36] Since these driving forces are more negative than −0.3 eV, the electron injection and dye-regeneration processes are energetically viable and sufficient (Table 1).[35] The above results clearly show that the dyes will be potentially efficient sensitizers for DSSCs. The schematic energy levels of **ICZ-Br**, **ICZ-TPA** and **ICZ-TMOP** based on absorption and electrochemical data are shown in Fig. 5.

Theoretical calculation

In order to visualize the effect of molecular structure and the electron distribution of **ICZ-Br**, **ICZ-TPA** and **ICZ-TMOP** on the performances of DSSCs, their geometries and energies were optimized by density functional theory (DFT) calculations at the B3LYP/6-31G(d) level. The molecular geometries and electronic distribution of the frontier molecular orbitals (HOMOs and LUMOs) of the presented dyes were computed and the results are displayed in Fig. 6. The HOMO of **ICZ-TPA** resides mainly on the π-conjugated indolo[3,2-*b*]carbazole donor, while the LUMO resides over the π-spacer thiophene and cyanoacrylic acid anchoring group, which leads to a strong electronic coupling with the TiO_2 surface and thus improves the electron injection efficiency. The calculated energy gaps (LUMO–HOMO) of the dyes **ICZ-Br**, **ICZ-TPA** and **ICZ-TMOP** are 2.05, 1.95 and 1.97 eV, respectively. The similar energy gaps are due to their similar electronic structure, which is in agreement with their similar absorption spectra and electrochemical results.

There is almost no HOMO delocalized on the second donor in dyes, which may be caused by the large dihedral angles between the indolo[3,2-*b*]carbazole plane and the adjacent phenylene plane. The phenylene units on the 6,12-positions of indolo[3,2-*b*]carbazole directly cause the coplanarity of the structure to be more twisted due to the high repulsion of charges between the H atom on the 2-ethylhexyl and the H atom on the adjacent phenylene. This twisted molecule configuration may help suppress the dye aggregation and improve their photovoltaic performances. However, it also destroys the conjugation between the second donor and the indolo[3,2-*b*]carbazole unit, and thus may affect the effective electron transfer in the dyes.

Photovoltaic properties

To optimize the DSSCs' performances, we first studied the effects of dye-adsorption solvent based on the dye **ICZ-TPA**.

The photovoltaic parameters in terms of short-circuit photocurrent density (J_{sc}), open circuit voltage (V_{oc}), fill factor (FF), and overall photoconversion efficiency (PCE) for each DSSC are summarized in Table 2. Although the V_{oc} based on different solvents change a little, the J_{sc} and PCEs values of the dye both increase in the order of DCM < DMF < toluene < THF. The dye uptake amounts of **ICZ-TPA** in DCM, DMF, toluene and THF solution are 3.18×10^{-7}, 3.32×10^{-7}, 3.25×10^{-7}, and 3.99×10^{-7} M cm^{-2}, respectively. Thus the higher dye uptake amount produces the larger J_{sc}. The best performances are achieved with the V_{oc} of 0.74 V, J_{sc} of 5.3 mA cm^{-2}, FF of 0.7 and PCE of 2.72%, by using THF as the dye-adsorption solvent.

By fixing THF as the dye-adsorption solvent, the DSSCs based on three dyes were prepared and characterized under standard AM 1.5 illumination (Fig. 7). The DSSCs based on **ICZ-TPA** show better performances than the other dyes, with higher J_{sc} and PCE, which may be attributed to the difference in the second donor unit in the dyes. **ICZ-TPA** contains a triphenylamine donor unit which has a stronger electron-rich ability than that of trimethoxyphenyl (**ICZ-TMOP**) and bromine (**ICZ-Br**), leading to stronger UV-vis absorption and larger photocurrent density. That also can evolve from the incident photo-to-electron conversion efficiency (IPCE) of the dyes.

As can be seen, the IPCE spectra of the DSSCs based on dyes exhibit photocurrent generations from 350 nm to 600 nm (Fig. 8) and the maximum IPCE values are all found at 420 nm, 65.4% for **ICZ-TPA**, 62.7% for **ICZ-TMOP** and 47.4% for **ICZ-Br**. Compared to **ICZ-Br**, the dyes **ICZ-TPA** and **ICZ-TMOP** show enhanced IPCE in the visible light range, reflecting higher light-harvesting ability and effective electron-injection from the excited dyes to the TiO_2 condition band.

Table 2 Effects of dye-adsorption solvent on the photovoltaic performances of DSSCs employing **ICZ-TPA** as sensitizer

Solvent	V_{oc} (V)	J_{sc} (mA cm^{-2})	FF	PCE (%)
DCM	0.74	4.50	0.74	2.47
DMF	0.72	5.01	0.69	2.48
Toluene	0.74	5.07	0.68	2.53
THF	0.74	5.30	0.70	2.72

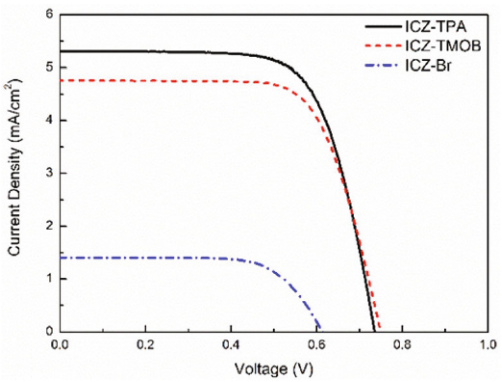

Fig. 7 *J*–*V* characteristics of DSSCs based on different dyes.

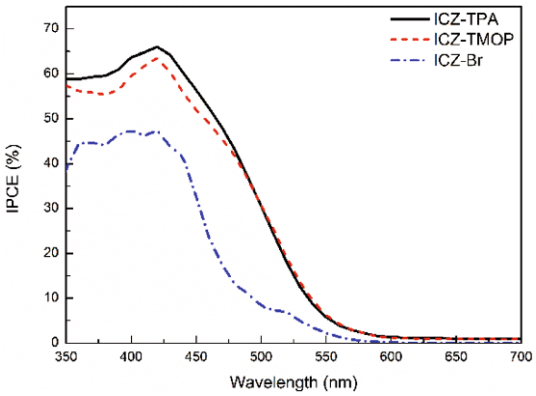

Fig. 8 IPCE spectra of DSSCs.

To further understand the electron transport properties, electrochemical impedance spectra (EIS) analysis was applied at an applied bias of about 0.7 V (equivalent to the open circuit voltage) (Fig. 9). The Nyquist plots usually show three semicircles located in high, middle and low frequency regions (from left to right), representing the impedances of the charge transfer (R_{ct}) on the Pt counter electrode, the charge recombination (R_r) on the interface of the TiO_2/dye/electrolyte, and the electrolyte diffusion, respectively.[37,38] As can be seen, the smaller semicircle in the low frequency region related to the electrolyte diffusion is not observed and overlapped by the larger semicircle in the middle frequency region. Fig. 9 revealed that the semicircle of the **ICZ-TMOP** electrode in the middle frequency region is larger than that of the **ICZ-TPA** and **ICZ-Br** electrodes, revealing an improvement in the retardation of charge recombination since that back electron recombination with I_3^- in the electrolyte is suppressed. This is in good agreement with the slightly high open circuit voltage of **ICZ-TMOP**. This indicates that the methoxyl units in the second donor of **ICZ-TMOP** are helpful for the suppression of dark current and improve the photovoltage.

In general, the utilization of chenodeoxycholic acid (CDCA) as co-adsorbent (simultaneously adsorbed on the TiO_2 electrode during the dye adsorption process) has been proved to

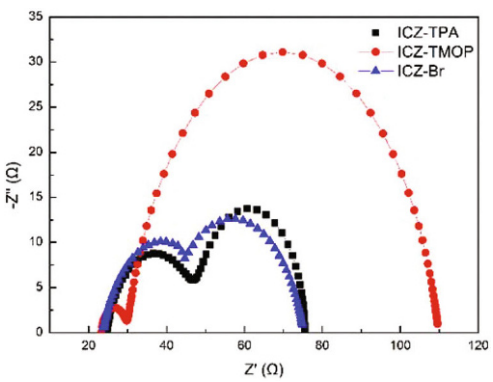

Fig. 9 EIS spectra of DSSCs.

Table 3 Photovoltaic performances of DSSCs based on **ICZ-TPA** and **ICZ-TMOP** with different concentration of CDCA as co-adsorbent

ICZ-Br (M)	**ICZ-TPA** (M)	**ICZ-TMOB** (M)	CDCA (mM)	V_{oc} (V)	J_{sc} (mA cm^{-2})	FF	PCE (%)
0	5×10^{-4}	0	0	0.74	5.3	0.70	2.72
			0.5	0.75	5.06	0.73	2.77
			1	0.75	5.69	0.72	3.11
			2	0.76	5.54	0.73	3.05
			4	0.75	5.22	0.74	2.91
			5	0.76	5.21	0.73	2.86
0	0	5×10^{-4}	0	0.75	4.76	0.70	2.5
			0.5	0.78	4.74	0.70	2.56
			1	0.75	5.09	0.74	2.83
			2	0.75	5.0	0.75	2.81
			4	0.75	4.95	0.71	2.64
			5	0.76	4.64	0.73	2.58
5×10^{-4}	0	0	0	0.61	3.89	0.69	1.65

be an efficient method to improve the DSSCs' performances, due to the suppression of dye aggregation and prevention of the backward electron transfer. Therefore, the effect of coadsorption of dye and CDCA was investigated by mixing various concentrations of CDCA with respective **ICZ-TPA** and **ICZ-TMOP** in the THF dye bath for fabricating sensitized TiO_2 films (Table 3).

As the concentration of CDCA increase from 0 to 1 mM, the J_{sc} of the dyes both increase, from 5.3 to 5.69 mA cm^{-2} for **ICZ-TPA**, and from 4.76 to 5.09 mA cm^{-2} for **ICA-TMOB**. The increased J_{sc} obviously stems from the coadsorption of CDCA, which weakens the intermolecular interactions and thus reduces the charge recombination rate in the DSSCs. The highest PCE values (3.11% for **ICZ-TPA**, and 2.83% for **ICA-TMOB**) are achieved at the CDCA concentration of only 1 mM. This CDCA concentration is particularly low compared with the values reported in literature,[14,39–41] suggesting that undesirable dye aggregates are effectively suppressed in the present DSSCs, presumably due to the strong steric hindrance caused by the 6,12-diphenyl substituted indolo[3,2-*b*]carbazole core. As the CDCA concentration increases to 5 mM, the J_{sc} and PCE values of the dyes both decrease to some extent, since the coadsorbed CDCA molecules occupy the binding sites on the TiO_2 film, leading to a decrease in the amount of organic dyes loaded on TiO_2. At the same CDCA concentration, the J_{sc} and PCE of **ICZ-TPA** are higher than that of **ICA-TMOB**, which can be mainly attributed to the good light-harvesting ability and electron injection efficiency. The **ICZ-TPA** dye has higher IPCE values from 350 nm to 500 nm, which ensure a high photocurrent. The difference of these dyes is the structure of the second donor. It is clear that the triphenylamine unit has stronger electron-donating ability and larger steric hindrance than trimethoxyphenylene and bromine. As a result, **ICZ-TPA** displays a higher HOMO, a narrower band gap, a broader IPCE, and higher J_{sc} and PCE.

Despite the considerable high open circuit voltages (V_{oc}) and fill factors (FF) for the present DSSCs, the low short-circuit photocurrent density (J_{sc}) results in the low photoconversion efficiency (PCE), which is probably due to the narrow absorption spectra. The results presented here suggest that indolo[3,2-*b*]carbazole could be a promising group to construct highly efficient organic dyes. Further work on the change in the substituted positions on indolo[3,2-*b*]carbazole or cosensitization with other dyes is also in progress for improving the photocurrent density.

Conclusions

In summary, we have designed and synthesized three types of novel D–D–π-A dyes (**ICZ-Br**, **ICZ-TPA** and **ICZ-TMOP**) by utilizing indolo[3,2-*b*]carbazole as first donor and bromine, triphenylamine and 3,4,5-trimethoxybenzene as second donor group, respectively, perpendicularly attached on the first donor. The second donor plays important roles in improving dye aggregation as well as tuning the photoelectronic properties. Results from absorption and photovoltaic properties demonstrate that these indolo[3,2-*b*]carbazole based dyes show good performances with high V_{oc} of 0.75 V, FF of 0.72, and a moderate PCE of 3.11% under AM 1.5 irradiation. Our study indicates that the incorporation of indolo[3,2-*b*]carbazole as a π-conjugated core into the dye backbone is a promising approach to constructing highly efficient D–D–π-A metal-free organic dyes.

Acknowledgements

The authors acknowledge the financial support by the National Nature Science Foundation of China (no. 21303256 and 11274347).

Notes and references

1 B. Liu and E. S. Aydil, Growth of oriented single-crystalline rutile TiO2 nanorods on transparent conducting substrates for dye-sensitized solar cells, *J. Am. Chem. Soc.*, 2009, **131**, 3985–3990.

2 A. Mishra, M. K. R. Fischer and P. Baeuerle, Metal-free organic dyes for dye-sensitized solar cells: from structure:

property relationships to design rules, *Angew. Chem., Int. Ed.*, 2009, **48**, 2474–2499.
3 M. K. Nazeeruddin, F. De Angelis, S. Fantacci, A. Selloni, G. Viscardi, P. Liska, S. Ito, T. Bessho and M. Gratzel, Combined experimental and DFT-TDDFT computational study of photoelectrochemical cell ruthenium sensitizers, *J. Am. Chem. Soc.*, 2005, **127**, 16835–16847.
4 M. Gratzel, The advent of mesoscopic injection solar cells, *Prog. Photovoltaics*, 2006, **14**, 429–442.
5 M. K. Nazeeruddin, S. M. Zakeeruddin, R. Humphry-Baker, M. Jirousek, P. Liska, N. Vlachopoulos, V. Shklover, C. H. Fischer and M. Gratzel, Acid–base equilibria of (2,2'-bipyridyl-4,4'-dicarboxylic acid)ruthenium(II) complexes and the effect of protonation on charge-transfer sensitization of nanocrystalline titania, *Inorg. Chem.*, 1999, **38**, 6298–6305.
6 X. Li, J. Gui, H. Yang, W. Wu, F. Li, H. Tian and C. Huang, A new carbazole-based phenanthrenyl ruthenium complex as sensitizer for a dye-sensitizd solar cells, *Inorg. Chim. Acta*, 2008, **361**, 2835–2840.
7 C. Y. Chen, S. J. Wu, C. G. Wu, J. G. Chen and K. C. Ho, A ruthenium complex with super-high light-harvesting capacity for dye-sensitized solar cells, *Angew. Chem., Int. Ed.*, 2006, **45**, 5822–5825.
8 X. Lu, Q. Feng, T. Lan, G. Zhou and Z.-S. Wang, Molecular engineering of quinoxaline-based organic sensitizers for highly efficient and stable dye-sensitized solar sells, *Chem. Mater.*, 2012, **24**, 3179–3187.
9 D. H. Lee, M. J. Lee, H. M. Song, B. J. Song, K. D. Seo, M. Pastore, C. Anselmi, S. Fantacci, F. De Angelis, M. K. Nazeeruddin, M. Graeetzel and H. K. Kim, Organic dyes incorporating low-band-gap chromophores based on π-extended benzothiadiazole for dye-sensitized solar cells, *Dyes Pigm.*, 2011, **91**, 192–198.
10 J. He, W. Wu, J. Hua, Y. Jiang, S. Qu, J. Li, Y. Long and H. Tian, Bithiazole-bridged dyes for dye-sensitized solar cells with high open circuit voltage performance, *J. Mater. Chem.*, 2011, **21**, 6054–6062.
11 J. Song, F. Zhang, C. Li, W. Liu, B. Li, Y. Huang and Z. Bo, Phenylethyne-Bridged Dyes for Dye-Sensitized Solar Cells, *J. Phys. Chem. C*, 2009, **113**, 13391–13397.
12 C.-Y. Chen, J.-G. Chen, S.-J. Wu, J.-Y. Li, C.-G. Wu and K.-C. Ho, Multifunctionalized ruthenium-based supersensitizers for highly efficient dye-sensitized solar cells, *Angew. Chem., Int. Ed.*, 2008, **47**, 7342–7345.
13 C. S. Karthikeyan, H. Wietasch and M. Thelakkat, Highly efficient solid-state dye-sensitized TiO2 solar cells using donor-antenna dyes capable of multistep charge-transfer cascades, *Adv. Mater.*, 2007, **19**, 1091–1095.
14 Q. Chai, W. Li, J. Liu, Z. Geng, H. Tian and W.-H. Zhu, Rational molecular engineering of cyclopentadithiophene-bridged D-A-π-A sensitizers combining high photovoltaic efficiency with rapid dye adsorption, *Sci. Rep.*, 2015, **5**, 11330.
15 Z. Ning, Q. Zhang, W. Wu, H. Pei, B. Liu and H. Tian, Starburst triarylamine based dyes for efficient dye-sensitized solar cells, *J. Org. Chem.*, 2008, **73**, 3791–3797.
16 T. Kaewpuang, N. Prachumrak, S. Namuangruk, S. Jungsuttiwong, T. Sudyoadsuk, P. Pattanasattayavong and V. Promarak, (D–π–)2D–π–A-Type organic dyes for efficient dye-sensitized solar cells, *Eur. J. Org. Chem.*, 2016, 2528–2538.
17 S. Fuse, R. Takahashi, M. M. Maitani, Y. Wada, T. Kaiho, H. Tanaka and T. Takahashi, Synthesis and evaluation of thiophene-based organic dyes containing a rigid and non-planar donor with secondary electron donors for use in dye-sensitized solar cells, *Eur. J. Org. Chem.*, 2016, 508–517.
18 S. Namuangruk, R. Fukuda, M. Ehara, J. Meeprasert, T. Khanasa, S. Morada, T. Kaewin, S. Jungsuttiwong, T. Sudyoadsuk and V. Promarak, D–D–π–A-Type organic dyes for dye-sensitized solar cells with a potential for direct electron injection and a high extinction coefficient: synthesis, characterization, and theoretical investigation, *J. Phys. Chem. C*, 2012, **116**, 25653–25663.
19 M.-D. Zhang, H.-X. Xie, X.-H. Ju, L. Qin, Q.-X. Yang, H.-G. Zheng and X.-F. Zhou, D-D-π-A organic dyes containing 4,4′-di(2-thienyl)triphenylamine moiety for efficient dye-sensitized solar cells, *Phys. Chem. Chem. Phys.*, 2013, **15**, 634–641.
20 G. Wu, F. Kong, J. Li, X. Fang, Y. Li, S. Dai, Q. Chen and X. Zhang, Triphenylamine-based organic dyes with julolidine as the secondary electron donor for dye-sensitized solar cells, *J. Power Sources*, 2013, **243**, 131–137.
21 T. Sudyoadsuk, S. Pansay, S. Morada, R. Rattanawan, S. Namuangruk, T. Kaewin, S. Jungsuttiwong and V. Promarak, Synthesis and characterization of D–D–π–A-Type organic dyes bearing carbazole–carbazole as a donor moiety (D–D) for efficient dye-sensitized solar cells, *Eur. J. Org. Chem.*, 2013, 5051–5063.
22 Z. Ning and H. Tian, Triarylamine: a promising core unit for efficient photovoltaic materials, *Chem. Commun.*, 2009, 5483–5495.
23 L.-L. Tan, J.-F. Huang, Y. Shen, L.-M. Xiao, J.-M. Liu, D.-B. Kuang and C.-Y. Su, Highly efficient and stable organic sensitizers with duplex starburst triphenylamine and carbazole donors for liquid and quasi-solid-state dye-sensitized solar cells, *J. Mater. Chem. A*, 2014, **2**, 8988–8994.
24 C. Teng, X. Yang, C. Yuan, C. Li, R. Chen, H. Tian, S. Li, A. Hagfeldt and L. Sun, Two novel carbazole dyes for dye-sensitized solar cells with open-circuit voltages up to 1 V based on Br–/Br3– electrolytes, *Org. Lett.*, 2009, **11**, 5542–5545.
25 G. Marotta, M. A. Reddy, S. P. Singh, A. Islam, L. Han, F. De Angelis, M. Pastore and M. Chandrasekharam, Novel carbazole-phenothiazine dyads for dye-sensitized solar cells: a combined experimental and theoretical study, *ACS Appl. Mater. Interfaces*, 2013, **5**, 9635–9647.
26 S. Cai, X. Hu, Z. Zhang, J. Su, X. Li, A. Islam, L. Han and H. Tian, Rigid triarylamine-based efficient DSSC sensitizers with high molar extinction coefficients, *J. Mater. Chem. A*, 2013, **1**, 4763–4772.
27 Y. Liang, B. Peng and J. Chen, Correlating dye adsorption behavior with the open-circuit voltage of triphenylamine-

based dye-sensitized solar cells, *J. Phys. Chem. C*, 2010, **114**, 10992–10998.

28 S. Chen, J. Wei, K. Wang, C. Wang, D. Chen, Y. Liu and Y. Wang, Constructing high-performance blue, yellow and red electroluminescent devices based on a class of multi-functional organic materials, *J. Mater. Chem. C*, 2013, **1**, 6594–6602.

29 H.-C. Ting, Y.-M. Chen, H.-W. You, W.-Y. Hung, S.-H. Lin, A. Chaskar, S.-H. Chou, Y. Chi, R.-H. Liu and K.-T. Wong, Indolo[3,2-b]carbazole/benzimidazole hybrid bipolar host materials for highly efficient red, yellow, and green phosphorescent organic light emitting diodes, *J. Mater. Chem.*, 2012, **22**, 8399–8407.

30 X. H. Zhang, Z. S. Wang, Y. Cui, N. Koumura, A. Furube and K. Hara, Organic Sensitizers Based on Hexylthiophene-Functionalized Indolo[3,2-b]carbazole for efficient Dye-Sensitized Solar Cells, *J. Phys. Chem. C*, 2009, **113**, 13409–13415.

31 H. Choi, C. Baik, S. O. Kang, J. Ko, M.-S. Kang, M. K. Nazeeruddin and M. Gratzel, Highly efficient and thermally stable organic sensitizers for solvent-free dye-sensitized solar cells, *Angew. Chem., Int. Ed.*, 2008, **47**, 327–330.

32 S. M. Zakeeruddin, M. K. Nazeeruddin, R. Humphry-Baker, P. Pechy, P. Quagliotto, C. Barolo, G. Viscardi and M. Gratzel, Design, synthesis, and application of amphiphilic ruthenium polypyridyl photosensitizers in solar cells based on nanocrystalline TiO2 films, *Langmuir*, 2002, **18**, 952–954.

33 T. Horiuchi, H. Miura, K. Sumioka and S. Uchida, High efficiency of dye-sensitized solar cells based on metal-free indoline dyes, *J. Am. Chem. Soc.*, 2004, **126**, 12218–12219.

34 T. Daeneke, T.-H. Kwon, A. B. Holmes, N. W. Duffy, U. Bach and L. Spiccia, High-efficiency dye-sensitized solar cells with ferrocene-based electrolytes, *Nat. Chem.*, 2011, **3**, 211–215.

35 T. Higashino, Y. Fujimori, K. Sugiura, Y. Tsuji, S. Ito and H. Imahori, Tropolone as a high-performance robust anchoring group for dye-sensitized solar cells, *Angew. Chem., Int. Ed.*, 2015, **54**, 9052–9056.

36 K. Kurotobi, Y. Toude, K. Kawamoto, Y. Fujimori, S. Ito, P. Chabera, V. Sundström and H. Imahori, Highly asymmetrical porphyrins with enhanced push–pull character for dye-sensitized solar cells, *Chem. – Eur. J.*, 2013, **19**, 17075–17081.

37 J. Nissfolk, K. Fredin, A. Hagfeldt and G. Boschloo, Recombination and transport processes in dye-sensitized solar cells investigated under working conditions, *J. Phys. Chem. B*, 2006, **110**, 17715–17718.

38 Q. Wang, Z. Zhang, S. M. Zakeeruddin and M. Grätzel, Enhancement of the performance of dye-sensitized solar cell by formation of shallow transport levels under visible light Illumination, *J. Phys. Chem. C*, 2008, **112**, 7084–7092.

39 Y. Wu and W. Zhu, Organic sensitizers from D–π-A to D–A-π-A: effect of the internal electron-withdrawing units on molecular absorption, energy Levels and photovoltaic performances, *Chem. Soc. Rev.*, 2013, **42**, 2039–2058.

40 Y. Wu, M. Marszalek, S. M. Zakeeruddin, Q. Zhang, H. Tian, M. Gratzel and W. Zhu, High-conversion-efficiency organic dye-sensitized solar cells: molecular engineering on D–A–π-A featured organic indoline dyes, *Energy Environ. Sci.*, 2012, **5**, 8261–8272.

41 S. W. Park, K.-I. Son, M. J. Ko, K. Kim and N.-G. Park, Effect of donor moiety in organic sensitizer on spectral response, electrochemical and photovoltaic properties, *Synth. Met.*, 2009, **159**, 2571–2577.